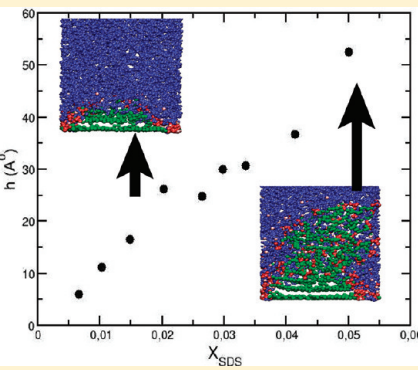


Structural Transition of the Sodium Dodecyl Sulfate (SDS) Surfactant Induced by Changes in Surfactant Concentrations

Hector Domínguez*

Instituto de Investigaciones en Materiales, UNAM, Universidad Nacional Autónoma de México, México, D.F. 04510

ABSTRACT: Molecular dynamics simulations were used to investigate aggregation of surfactants at the solid–liquid interface at different surfactant concentrations. For these studies simulations of the sodium dodecyl sulfate (SDS) surfactant with a graphite surface were carried out. At low concentrations the SDS molecules aggregated in slices of cylinders attached to the solid surface, whereas at slightly higher concentrations the structures showed irregular shapes. When the concentration was again increased to a higher value, the molecules aggregated in a more complex structure, an irregular aggregate on the top of a semicylinder adsorbed on the graphite surface. From the present results more insights about the internal structure of the aggregates were observed than in actual experiments, e.g., it was found that the SDS tails arrayed in well-defined layers close to the graphite surface. Moreover, from the internal structure it was possible to show a structural transition driven by an increment in the surfactant concentration which, to the best of our knowledge, has not been studied from a molecular point of view. Therefore the transition was studied in terms of the height of the structures. Along with these studies adsorption of the aggregates, by calculating contact angles, and adsorption isotherms were also analyzed. Finally, investigations of the surface coverage with the concentration showed that this quantity did not change considerably with the concentration.



1. INTRODUCTION

Surfactants at interfaces have been investigated not only for their scientific interest but also for their applicability in industrial processes such as detergency, lubrication, and colloid stabilization. Several experiments have been conducted to study the behavior of surfactants at liquid/air and liquid/liquid interfaces;^{1–8} however, surfactants at liquid/solid interfaces have been less understood despite of their interest in areas such as adsorption, electrochemistry or electrode surfaces.⁹

Nowadays, the formation of spheres, cylinders, and bilayers in bulk solutions is well-known; however, how aggregation is modified by the presence of solid surfaces is still a matter of continue investigations. Although some experiments suggest that most of the aggregates observed in bulk can also appear at the solid/liquid interface,^{9–14} the nature, the structure, and the shape of these aggregates present different features due to the extra solid–surfactant interaction.^{15,16}

A valuable technique to study the self-assembly of surfactants adsorbed from aqueous solution on different solid surfaces has been atomic force microscopy (AFM).^{9,13,17–21} For instance, from AFM experiments, it is possible to observe how surfactant concentration affects aggregation or the effects on aggregation by adding salt to the system.²² The effects of the chain length¹² and the role of the surfactant headgroups¹⁸ in the self-assembly of surfactant molecules have been also investigated. On the other hand, ellipsometry techniques have also been very useful to study adsorption and measurements of film thickness of surfactants on solid surfaces.^{23–25}

Therefore, several studies on different hydrophobic and hydrophilic surfaces, such as graphite, silica, mica, gold, etc., have been conducted.^{16,19,26,27} In particular, hydrophobic substrates have been investigated and people have observed the formation of semicylindrical aggregates caused by the interactions with the tail groups through the van der Waals forces.^{13,22,28} On the other hand few studies in bulk have been conducted to study transitions on surfactant molecules and they have observed structural changes^{29–32} and reorganization of molecular forms on solid surfaces.¹⁴

Due to the complexity of these problems, an alternative tool to study such interfacial systems has appeared: computer simulations. Therefore, simulations from fully atomistic^{33–36} to coarse-grain models^{37–41} have been reported in the literature. In particular dissipative particle dynamics (DPD) is a technique that allows us to work large scales of time and sizes and it has been used to study, for instance, self-assembly of surfactants around carbon nanotubes.^{42,43} More over, people have also investigated formation of structures depending on the alkyl chain length. They observed that surfactants with short chains form monolayers, whereas surfactants with long tails form semicylinders on a graphite surface. However, from classical molecular dynamics simulations people have observed spherical and hemicylindrical shapes of surfactants at water/silica and water/graphite

Received: March 25, 2011

Revised: September 15, 2011

Published: September 16, 2011

interfaces.^{44,45} Other groups have studied the role of counterions of anionic surfactants on graphite surfaces^{46,47} and the curvature effects of surfactant adsorption,⁴⁸ whereas some other works have investigated orientation of surfactants on a graphite surface which could explain the formation of semicylinder aggregates on the plate.^{49,50}

In a previous work we studied the formation of semicylinders on a graphite surface at low concentration, and we characterized their structures.³⁶ In the present paper studies about the formation of surfactant aggregates from low to high concentrations are investigated. While experiments can provide some information about surfactant adsorption, they just provide little information about the internal or microscopic structure of the aggregates at the solid surface. Here, we show a structural transition on the surface produced by increments of the surfactant concentration which is accompanied by a change in the number of surfactant layers adsorbed on the surface. Finally we also constructed an adsorption isotherm with the concentration.

2. COMPUTATIONAL METHOD AND MODEL

Simulations were conducted on the anionic sodium dodecyl sulfate (SDS) molecule with a model of a hydrocarbon chain of 12 united carbon atoms attached to a headgroup, SO_4^- . The simulation parameters for the SDS were the same used in previous works.^{51,52} For the liquid phase we used the SPC water model, and for the solid surface we constructed two layers of graphite plates using an atomistic model.

The initial configuration was prepared from a monolayer of surfactant molecules, in all-trans configuration, with the SDS head groups initially pointed to the solid plate and placed close to the graphite surface of dimensions X and $Y = 40.249 \text{ \AA}$. Then 2416 water molecules and sodium cations (Na^+) were added to the system. The usual periodic boundary conditions were imposed, however, to prevent the formation of a second water/solid interface due to the periodicity of the system the z -dimension of the box was set to 150 \AA , i.e. a liquid/vapor interface was present at one end of the simulation box. The same procedure was carried out for nine different SDS concentrations (different number of SDS molecules), $X = 0.0066, 0.0104, 0.0149, 0.0203, 0.0265, 0.0298, 0.0335, 0.0414$, and 0.0501 cc , where concentration in this study refers to the number of SDS molecules divided by the total number of water molecules.

All simulations were carried out with the DL-POLY package⁵³ in the NVT ensemble at temperature of $T = 298 \text{ K}$ with a time step of 0.002 ps using the Hoover-Nose thermostat with relaxation time of 0.2 ps .⁵⁴ Long range electrostatic interactions were handled with the particle mesh Ewald method with precision of 10^{-4} and the van der Waals interactions were cut off at 10 \AA . Finally, long simulations were conducted up to 55 ns where the last 5 ns were used for data acquisition and configurational energy was monitored as a function of time to determine when systems reached equilibrium.

Because changes and fluctuations in the shape of micelles and surfactant aggregation occur in order of microseconds, these times scales might be too short to entirely describe the properties of the surfactants; nevertheless, we believe these simulations can provide dynamical information about the surfactant structures which is representative of the processes occurring in the systems.

3. RESULTS

In this section we present the calculations performed on the SDS surfactant for the nine different concentrations, $X = 0.0066,$

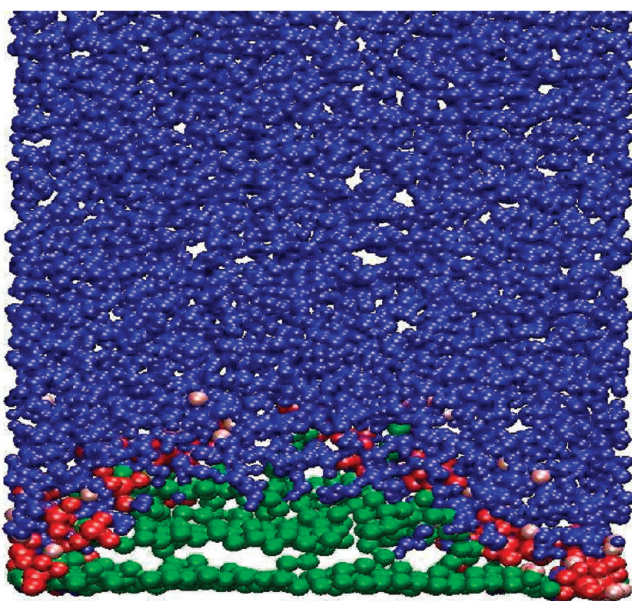


Figure 1. Snapshot of the SDS surfactant on a graphite surface at concentration of 0.0149 cc . Water is shown in blue, SDS headgroups in red, SDS tails in green, and the Na^+ counterions in pink. The graphite plate is located at the bottom of the molecules.

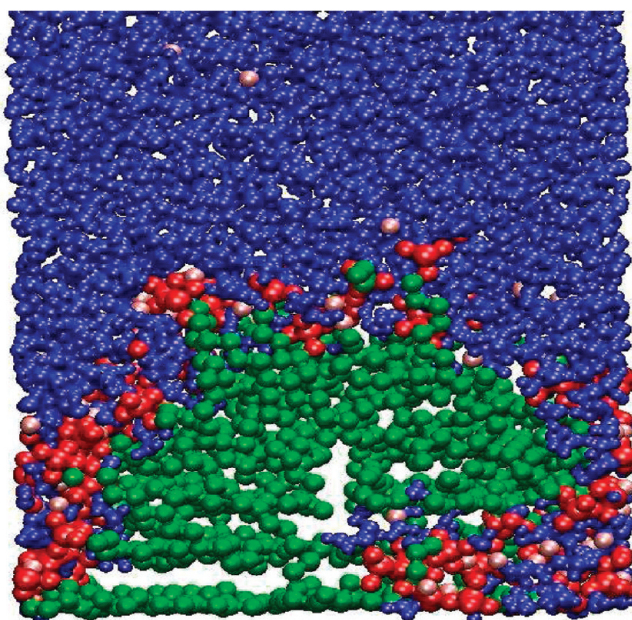


Figure 2. Snapshot of the SDS surfactant on a graphite surface at concentration of 0.0335 cc . Water is shown in blue, SDS headgroups in red, SDS tails in green, and the Na^+ counterions in pink. The graphite plate is located at the bottom of the molecules.

$0.0104, 0.0149, 0.0203, 0.0265, 0.0298, 0.0335, 0.0414$, and 0.0501 cc . Studies of the internal structure and how the SDS is adsorbed at the liquid/solid interface are discussed.

3.1. Surfactant Structure at the Interface. In all simulations it was observed that most of the head-groups close to the graphite were repelled leaving the tails close to the solid surface. Then, affinity between the graphite atoms with the carbons in the tails

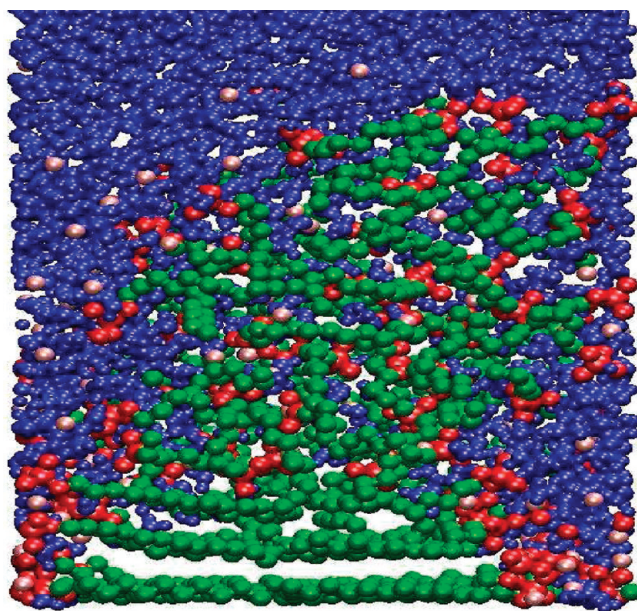


Figure 3. Snapshot of the SDS surfactant on a graphite surface at concentration of 0.0501 cc. Water is shown in blue, SDS headgroups in red, SDS tails in green, and the Na^+ counterions in pink. The graphite plate is located at the bottom of the molecules.

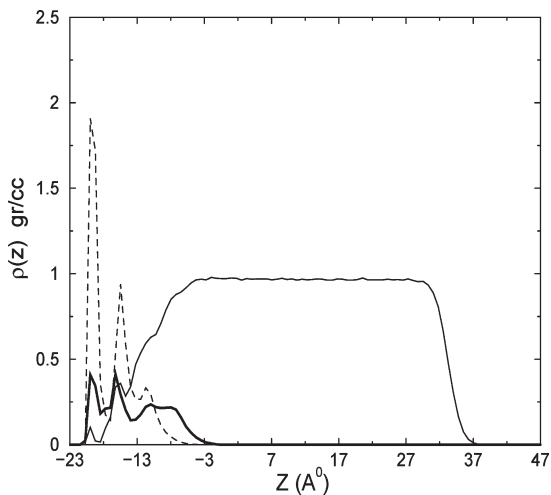


Figure 4. Typical density profiles for the SDS molecules on a graphite surface at concentration of 0.0149 cc. Water is depicted by the light solid line, the SDS head groups by the dark solid line and the SDS tails by the dashed line. The graphite surface is located at the left of the plot.

made the last groups to be adsorbed on the solid plate. At the lowest concentration it was possible to observe all SDS molecules adsorbed on the surface. As the concentration increased ($X < 0.0298$) the molecules self-organized to form cylinder slices attached on the graphite plate (Figure 1) which were named semicylinders to be consistent with the term used in experiments. These kind of structures were found in previous works and they were also observed by actual experiments.^{13,28,36} When the SDS concentration was increased ($X = 0.0335$ and 0.0414 cc), we did not observe regular structures, i.e., it was not possible to associate semicylinder shapes to those aggregates even when the systems were ran for longer time; that is, the structures remained with the

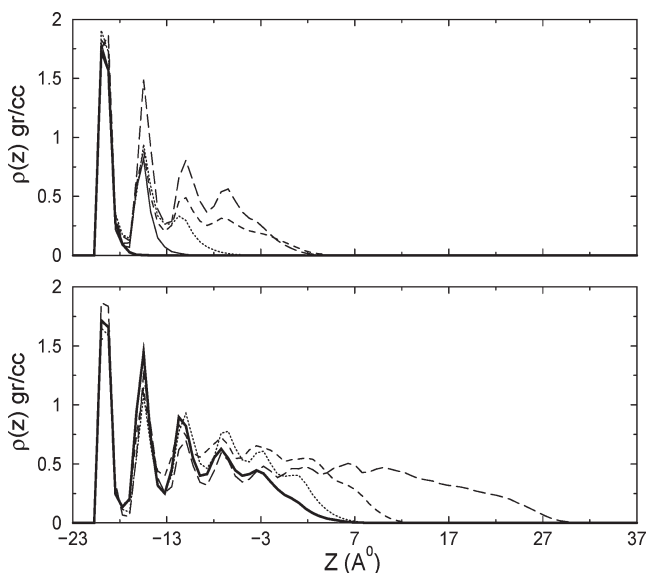


Figure 5. (Top) Density profiles for the SDS tails on a graphite surface at concentrations of 0.0066, 0.0104, 0.0149, 0.0203, and 0.0265 cc. (Bottom) Density profiles for the SDS tails on a graphite surface at concentrations of 0.0298, 0.0335, 0.0414, and 0.0501 cc.

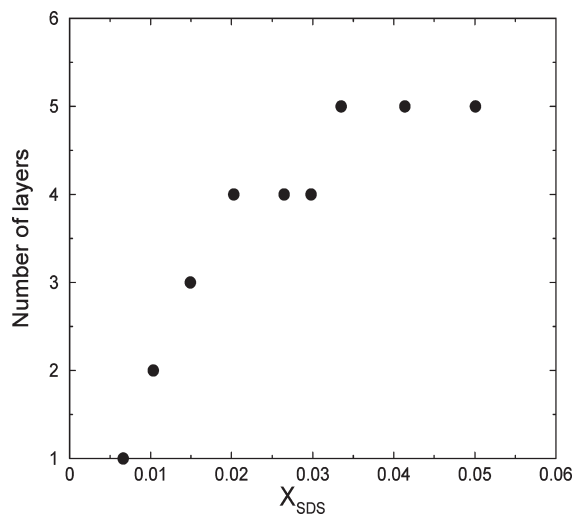


Figure 6. Number of SDS layers at each concentration.

same undefined shapes (Figure 2). However, at the highest concentration ($X = 0.0501$ cc), the molecules arrayed in a different structure; a structure which looks-like an irregular aggregate above of a semicylinder (Figure 3).

A general feature in all of the structures is the formation of well-defined layers composed of SDS tails adsorbed on the surface in agreement with previous simulations.^{36,46,52} However, at high concentrations, the layering structure disappeared far from the surface. The formation of layers close to the surface can be depicted from the density profiles calculated in the z -direction, i.e. normal to the liquid/solid interface. In Figure 4, typical z -dependent density profiles for the water, the headgroups and the hydrocarbon tails are shown. In Figure 5, density profiles of the tails only are also shown for all the systems (concentrations) where it was observed the formation of layers close to the surface

whereas at high concentrations those layers were less pronounced or they vanished far from the surface.

In Figure 6 is plotted the number of layers (obtained from Figure 5) in each aggregate as a function of the surfactant concentration. It was observed that the number of layers increased as the concentration increased until four layers were formed at concentration of 0.0203 cc and the same number of layers remained up to the concentration of 0.0298 cc. Then, at higher concentrations another layer was developed (i.e., five layers were observed), although it was not very sharp. It was interesting to note the same number of layers at concentrations between 0.0203 and 0.0298 cc, however, it was also noted that the change from four to five layers (at concentration of 0.0335 cc) corresponded to the case where the semicylinders lost their structures.

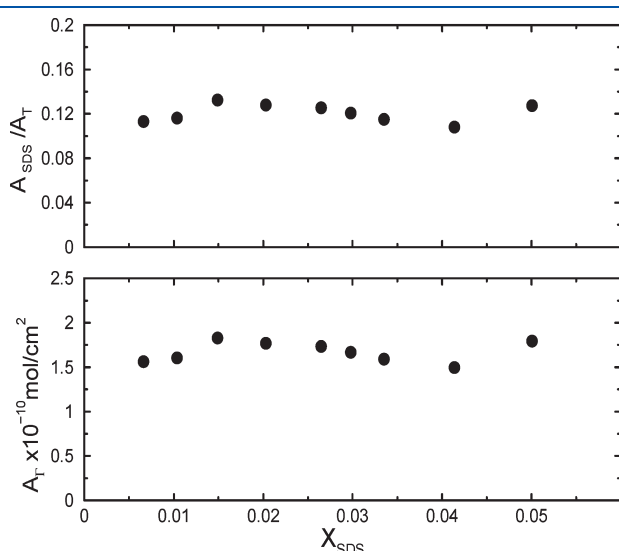


Figure 7. (Top) Ratio of the areas of the molecules adsorbed (in the first layers) on the surface with the total area of the graphite surface. (Bottom) Surface concentration of SDS molecules (in the first adsorbed layer) on the graphite surface.

Surface coverage was studied by the relation between the surface area occupied by the SDS molecules in the first adsorbed layer and the total area of the solid surface (top of Figure 7) and by the surface concentration (in mol cm^{-2} , bottom of Figure 7) where it was observed that the amount of adsorbed molecules on the surface was the same regardless the SDS concentration. It is also possible to obtain the same information from the snapshots in Figure 8. In Figure 8, panels a (at the lowest concentration) and b (at the highest concentration), we observed the same number of surfactant molecules deposited on the solid surface. However, in the first figure those molecules corresponded to the total number of molecules whereas in the other figure there were only some of the total molecules. These results suggested again that the amount of SDS molecules in the first adsorbed layer did not change significantly with concentration.

Adsorption of the molecules was calculated by the excess mass on the surface respect with the total mass by using the following equation:

$$\Gamma = \frac{m_t - m_p}{m_t} \quad (1)$$

where m_p denotes the mass of particles in the first adsorbed layer calculated from the density profiles (Figure 5) and m_t is the total mass of all SDS molecules. In Figure 9 the adsorption isotherm is plotted as a function of the concentration where the solid line is the fitting curve to the data using the Langmuir model

$$\Gamma = \Gamma_0 \frac{K_L(X - X_0)}{1 + K_L(X - X_0)} \quad (2)$$

where K_L is the Langmuir constant and X is the concentration of SDS surfactant in the system. X_0 corresponds to the lowest value of X and it was used to have a better fitting of the data. In the present work the maximum adsorption was approximated by taking the value of the surface concentration at the highest surfactant concentration (from Figure 7) and it was found a value of $5 \times 10^{-4} \text{ mol/g}$. On the other hand, from Figure 9 it was also obtained a Langmuir constant of $K_L = 139.35$ which gave us a Gibbs free energy of adsorption of $G_{\text{ads}} = -RT \ln K_L = -12.2 \text{ KJ/mol}$;

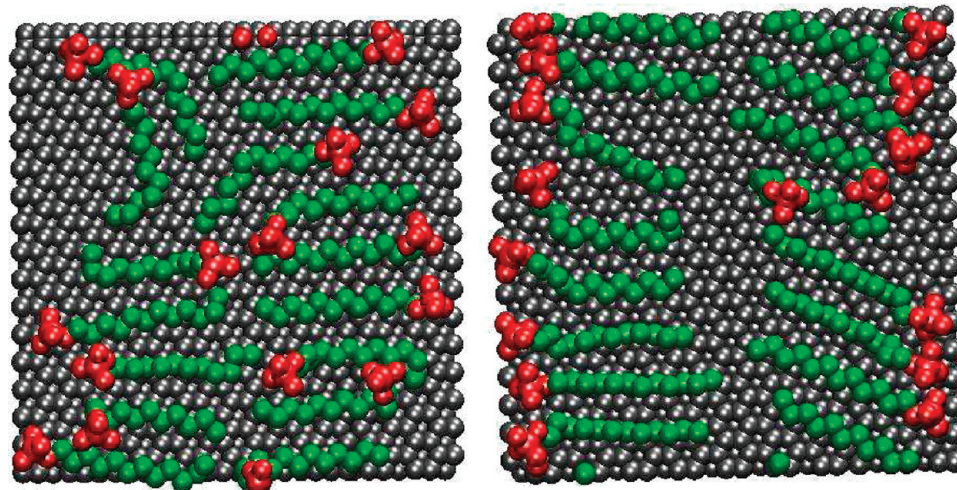


Figure 8. Snapshots of the first layer adsorbed on a graphite surface at concentrations of (a) 0.0066 and (b) 0.0501 cc. For better visualization the periodic boundary conditions were not removed, therefore some molecules seem to be broken. The graphite atoms are shown in gray whereas the rest of the molecules have the same colors as in Figure 1.

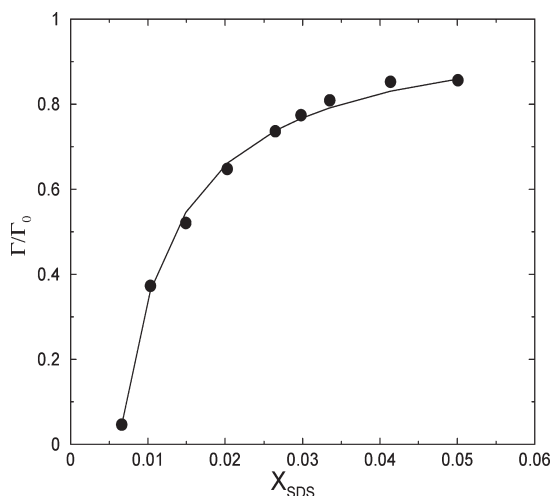


Figure 9. Adsorption isotherm of SDS on graphite. The solid line was obtained by fitting the Langmuir model to the data.

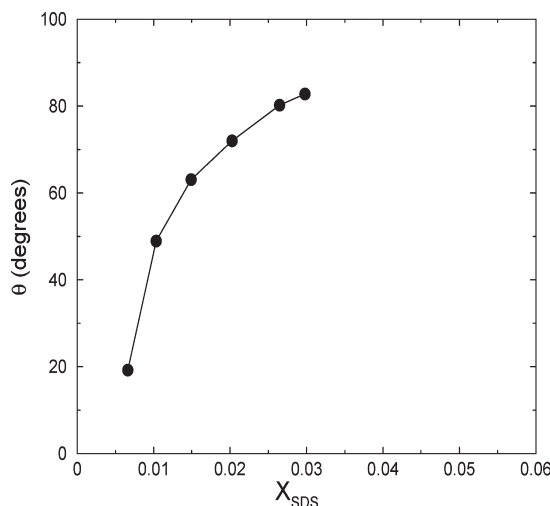


Figure 10. Contact angle calculations of the SDS aggregates, for different concentrations, adsorbed on the solid graphite plate.

values in the range of $G_{\text{ads}} = -10$ to -35 KJ/mol for the Gibbs free energy of micellization have been reported.^{55–58}

Adsorption of the aggregates was also characterized in terms of contact angles which were calculated by fitting a circle $[(X - X_0)^2 + (Z - Z_0)^2 = R^2]$ to the headgroups positions of the SDS molecules (mainly the sulfur atoms). Once the best fitting was obtained the slope of the curve at the position where the circle hit the graphite plane was calculated. Then, the contact angle was obtained as an average over twenty different configurations. It was observed an increment of the contact angle as the concentration increased until it reached the concentration of 0.0298 cc. As stated before (from concentrations above this value, 0.0335 and 0.0414 cc) the aggregate shapes were not well-defined, so it was difficult to calculate the contact angle. At concentration of 0.0149 cc which corresponds to a surface coverage of 45 \AA/molecule which is the area per headgroup at the critical micelle concentration at the water/air interface,⁵⁹ we found an angle of $\sim 60^\circ$ which it was similar to the angle found in previous simulations.⁴⁶ Data of contact angles are given in Figure 10. Simulations

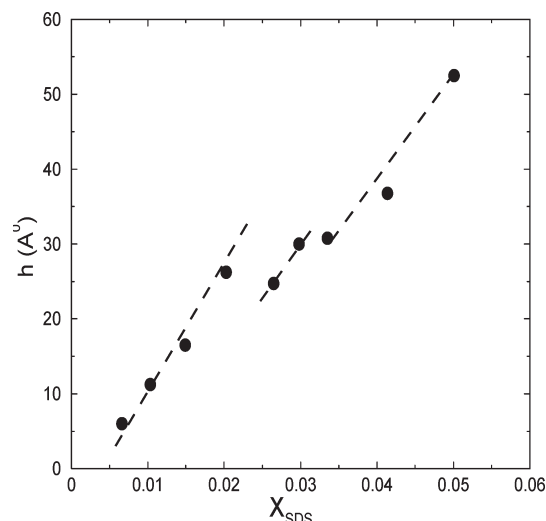


Figure 11. Plot of the heights of all structures for all concentrations. Dotted lines are just to guide the data and to show the discontinuities in the points.

in a larger area were conducted, i.e. $X = Y = 55.0 \text{ \AA}$ for a system with surfactant concentration of 0.0265 cc and a contact angle of 61° was estimated. In terms of area per headgroup this system corresponded to the one simulated previously at concentration 0.0149 cc; that is, they have an area per headgroup of 47.3 and $45 \text{ \AA}^2/\text{molecule}$, respectively. Therefore, the data calculated with the larger area systems is in agreement with those results.

Changes in the aggregate shapes suggest the system undergoes to a structural transition as the surfactant concentration increases. A common way to study transitions is by a Clausius–Clapeyron equation where the transition can be characterized by a discontinuous jump of an order parameter. In the present work we considered the height of the aggregates (h) as the order parameter. In Figure 11 a plot of the aggregate heights as a function of the surfactant concentration is shown. The height of the structures was obtained from the density profiles by measuring the distance from the first to the last points in the headgroup profiles. Experiments of the same system (SDS on graphite) have been conducted using the AFM technique; they observed similar structures (semicylinders), and they determined a height of 17 \AA for those aggregates.²² Other experiments, using ellipsometry, on a different surface, platinum, have found thickness of the adsorbed layer between 10 and 15 \AA .²³ Here, in this work at concentration of 0.0149 cc ($45 \text{ \AA}/\text{molecule}$, the area per headgroup at the critical micelle concentration at the water/air interface) we found a height of 16.5 \AA which is in good agreement with the experimental results.

From the same Figure 11 it was possible to observe a discontinuous jump in the parameter (h) at concentrations between 0.0203 and 0.0265 cc and also a small jump from concentration 0.0298 cc to concentration 0.0335 cc which suggested a possible change in the surfactant structure, nevertheless structures in this interval did not present regular shapes so it was possible they were in a metastable state. It is worthy to mention that the values of concentrations where the parameter h changed corresponded to those values where the number of internal layers also changed as depicted in Figure 6.

4. DISCUSSION AND CONCLUSIONS

By conducting molecular dynamics simulations we studied aggregation of the SDS surfactant on a graphite surface at different

surfactant concentrations. The first feature to note is that regardless the surfactant concentration the SDS tails always form layers close to the graphite plate. The number of layers increased with the concentration, however, at high concentrations the layering structure vanished far from the graphite surface. By considering that the tails are formed by carbon atoms and that the main potential with the graphite atoms comes from van der Waals interactions it was an expected result as discussed in a previous paper.⁴⁶ At the lowest concentration all SDS molecules were adsorbed on the surface whereas at intermediate concentrations it was possible to distinguish semicylinder-like structures. However, not only we observed the semicylindrical shapes but we also observed that the shapes were slices of cylinders which did not include the radius of the enclosing circles. It was also found that the tails did not array radially inside the semicylinders in agreement with our previous works.^{36,46} At higher concentrations the aggregate lost its semicylindrical shape until the concentration was increased again and a more complex structure was observed.

In fact the aggregate at the highest concentration (0.0501 cc) present a strange structure and it was not possible to corroborate it with direct experimental evidence. Therefore, different simulations at this concentration, using two different initial conditions were carried out to see if the structure was modified. In any case the final structure was not exactly the same found previously, however, it was possible to identify that the molecules aggregated with the same picture, i.e. there were adsorbed molecules on the graphite surface with other surfactants over those molecules. When the heights of these new structures were calculated in the same way as the original one (from the density profiles) it was found values around 50 Å which were of the same order of the number found in Figure 11. Unfortunately, we did not find experimental results at this high concentration in terms of structures to compare our results. However, it has been observed that the size of aggregates increases with concentration⁶⁰ and in reference²² the authors, working with a similar system (SDS on graphite) mentioned that they found a micellar aggregate diameter of ~50 Å at 81 mM which it is above the surface aggregation where they started observing formation of structures in their systems (2.8 mM).

However, the fact that for these simulations the final structure shapes were not exactly the same of that found in the original simulation might suggest that at this concentration the systems did not reach the final equilibration. Therefore, it is worthy to mention that results at this concentration should be taken with caution if we try to associate this structure with any real experimental structure.

The present results suggest the system undergoes to a structural transition characterized by a jump in the height of the aggregates which is also accompanied by a change in the number of layers inside the aggregates.

The adsorption of the aggregates were studied in terms of contact angles of the semicylinders and it was found that the aggregate contact angle decreased with the concentration. An isotherm adsorption was also constructed as a function of the concentration and it was found that it followed the Langmuir model where the inflection to the plateau of maximum adsorption occurred nearly at the concentration where the aggregate lost its semicylindrical structure.

AUTHOR INFORMATION

Corresponding Author

*E-mail: hectordc@servidor.unam.mx

ACKNOWLEDGMENT

I acknowledge support from DGTIC-UNAM by using the KanBalam supercomputer. I also thank all of the reviewers for their valuable comments to improve the manuscript.

REFERENCES

- (1) Saccani, J.; Castano, S.; Beaurein, F.; Laguerre, M.; Desbat, B. *Langmuir* **2004**, *20*, 9190.
- (2) Piasecki, D. A.; Wirth, M. J. *J. Phys. Chem.* **1993**, *97*, 7700.
- (3) Tian, Y.; Umemura, J.; Takenaka, T. *Langmuir* **1988**, *4*, 1064.
- (4) Higgins, D. A.; Naujok, R. R.; Corn, R. M. *Chem. Phys. Lett.* **1993**, *213*, 485.
- (5) Conboy, J. C.; Messmer, M. C.; Richmond, G. *Langmuir* **1998**, *14*, 6722.
- (6) Zhang, Z. H.; Tsuyumoto, I.; Kitamori, T.; Sawada, T. *J. Phys. Chem. B* **1998**, *102*, 10284.
- (7) Lytle, D. J.; Lu, J. R.; Su, T. J.; Thomas, R. K.; Penfold, J. *Langmuir* **1995**, *11*, 1001.
- (8) Lu, J. R.; Hromadova, M.; Simister, E. A.; Thomas, R. K.; Penfold, J. *J. Phys. Chem.* **1994**, *98*, 11519.
- (9) Jaschke, M.; Butt, H.-J.; Gaub, H. E.; Manne, S. *Langmuir* **1997**, *13*, 1381.
- (10) Grant, L. M.; Tiberg, F.; Ducker, W. A. *J. Phys. Chem. B* **1998**, *102*, 4288.
- (11) Ducker, W. A.; Wanless, E. J. *Langmuir* **1999**, *15*, 160.
- (12) Ducker, W. A.; Grant, L. M. *J. Phys. Chem. B* **1996**, *100*, 11507.
- (13) Manne, S.; Cleveland, J. P.; Gaub, H. E.; Stucky, G. D.; Hansma, P. K. *Langmuir* **1994**, *10*, 4409.
- (14) Tsukruk, V. V.; Genson, K.; Peleshanko, S.; Markutsya, S.; Lee, M.; Yoo, Y.-S. *Langmuir* **2003**, *19*, 495.
- (15) Li, L.; Wang, Y.; Vigild, M. E.; Ndoni, S. *Langmuir* **2010**, *26*, 13457.
- (16) Wolgemuth, J. L.; Workman, R. K.; Manne, S. *Langmuir* **2000**, *16*, 3077.
- (17) Manne, S.; Gaub, H. E. *Science* **1995**, *270*, 1480.
- (18) Patrick, H. N.; Warr, G. G.; Manne, S.; Aksay, I. A. *Langmuir* **1997**, *13*, 4349.
- (19) Tilberg, F.; Jonsson, B.; Tang, J.; Lindmann, B. *Langmuir* **1994**, *10*, 2294.
- (20) Lau, C.; Furlong, D. N.; Healy, T. W.; Grieser, F. *Colloids Surf. B* **1986**, *18*, 93.
- (21) Binning, G.; Quate, C. F.; Gerber, Ch. *Phys. Rev. Lett.* **1986**, *56*, 930.
- (22) Wanless, E. J.; Ducker, W. A. *J. Phys. Chem.* **1996**, *100*, 3207.
- (23) Besio, G. J.; Prudhomme, R. K.; Benziger, J. B. *Langmuir* **1988**, *4*, 140.
- (24) Rojas, O. J.; Neuman, R. D.; Claesson, P. M. *J. Colloid Interface Sci.* **2001**, *237*, 104.
- (25) Beaglehole, D.; Webster, B.; Werner, S. *J. Colloid Interface Sci.* **1998**, *202*, 541.
- (26) Schniepp, H. C.; Shum, H. C.; Saville, D. A.; Aksay, I. A. *J. Phys. Chem. C* **2008**, *112*, 14902.
- (27) Nakamura, H.; Sakai, H.; Aoshima, S.; Abe, M. *J. Oleo Sci.* **2002**, *51*, 781.
- (28) Yeo, Y. H.; Yackoboski, K.; McGonigal, G. C.; Thompson, D. J. *J. Vac. Sci. Technol.* **1992**, *A10*, 600.
- (29) Singh, T.; Drechsler, M.; Mueller, A. H. E.; Mukhopadhyay, I.; Kumar, A. *Phys. Chem. Chem. Phys.* **2010**, *12*, 11728.
- (30) Chaudhuri, A.; Halder, S.; Chattopadhyay, A. *Biochim. Biophys. Research Commun.* **2009**, *390*, 728.
- (31) Heerklotz, H.; Tsamaloukas, A.; Kita-Tokarczyk, K.; Strunz, P.; Gutberlet, T. *J. Am. Chem. Soc.* **2004**, *126*, 16544.
- (32) Narayanan, J.; Mendes, E.; Manohar, C. *Int. J. Mod. Phys. B* **2002**, *16*, 375.
- (33) Krishnan, M.; Balasubramanian, S. *Phys. Chem. Chem. Phys.* **2005**, *7*, 2044.

- (34) Bandyopadhyay, S.; Shelley, J. C.; Tarek, M.; Moore, P. B.; Klein, M. L. *J. Phys. Chem. B* **1998**, *102*, 6318.
- (35) Werder, T.; Walther, J. H.; Jaffe, R. L.; Halicioglu, T.; Koumoutsakos, P. *J. Phys. Chem. B* **2003**, *107*, 1345.
- (36) Dominguez, H. *J. Phys. Chem. B* **2007**, *111*, 4054.
- (37) Srinivas, G.; Nielsen, S. O.; Moore, P. B.; Klein, M. L. *J. Am. Chem. Soc.* **2006**, *128*, 848.
- (38) Kranenburg, M.; Venturoli, M.; Smit, B. *J. Phys. Chem. B* **2003**, *107*, 11491.
- (39) Goetz, R.; Gompper, G.; Lipowsky, R. *Phys. Rev. Lett.* **1999**, *82*, 221.
- (40) Shelley, J. C.; Shelley, M.; Reeder, R.; Bandyopadhyay, S.; Klein, M. L. *J. Phys. Chem. B* **2001**, *105*, 4464.
- (41) Tian, F.; Luo, Y.; Zhang, X. *J. Chem. Phys.* **2010**, *133*, 144701.
- (42) Calvaresi, M.; Dallavalle, M.; Zerbetto, F. *Small* **2009**, *5*, 2191.
- (43) Angelikopoulos, P.; Bock, H. *J. Phys. Chem. B* **2008**, *112*, 13793. *J. Phys. Chem. B* **2009**, *113*, 9350.
- (44) Shah, K.; Chiu, P.; Sinnott, S. B. *J. Colloid Interface Sci.* **2006**, *296*, 342.
- (45) Shah, K.; Chiu, P.; Jain, M.; Fortes, J.; Moudgil, B.; Sinnott, S. B. *Langmuir* **2005**, *21*, 5337.
- (46) Dominguez, H. *Langmuir* **2009**, *25*, 9006.
- (47) Tummala, N. R.; Striolo, A. *J. Phys. Chem. B* **2008**, *112*, 1987.
- (48) Tummala, N. R.; Striolo, A. *Phys. Rev. E* **2008**, *80*, 021408.
- (49) Sammalkorpi, M.; Panagiotopoulos, A. Z.; Haataja, M. *J. Phys. Chem. B* **2008**, *112*, 2915.
- (50) Sammalkorpi, M.; Panagiotopoulos, A. Z.; Haataja, M. *J. Phys. Chem. B* **2008**, *112*, 12954.
- (51) Schweighofer, K. J.; Essmann, U.; Berkowitz, M. *J. Phys. Chem. B* **1997**, *101*, 3793.
- (52) Dominguez, H.; Rivera, M. *Langmuir* **2005**, *21*, 7257.
- (53) Forester, T. R.; Smith, W. *DL-POLY Package of Molecular Simulation*; CCLRC, Daresbury Laboratory: Daresbury, U.K., 1996.
- (54) Hoover, W. G. *Phys. Rev. A* **1985**, *31*, 1695.
- (55) Liu, T. Q. *J. Dispersion Sci. Technol.* **2008**, *29*, 335.
- (56) Zana, R. *Langmuir* **1996**, *12*, 1208.
- (57) Valente, A. J. M.; Burrows, H. D. *J. Colloid Interface Sci.* **2008**, *323*, 141.
- (58) Szymczyk, K.; Janczuk, B. *Langmuir* **2009**, *25*, 4377.
- (59) Lu, J. R.; Marroco, A.; Su, T. J.; Thomas, R. K.; Penfold, J. *J. Colloid Interface Sci.* **1993**, *158*, 303.
- (60) Hayter, J. B. In *Proceeding of the International School of Physics: Physics of Amphiphiles: Micelles, Vesicles and Microemulsions*; Degiorgio, V., Ed.; Elsevier: Amsterdam, 1985; pp 59–93.